Optical near-field mapping with a superconducting nanowire detector

Karol Luszcz, Eric Bonvin, and Lukas Novotny
Photonics Laboratory, ETH Zürich, 8093 Zürich, Switzerland

(Received 30 April 2018; accepted 18 June 2018; published online 2 July 2018)

Optical near-fields are interesting from a theoretical perspective and of importance for practical applications, such as high-resolution imaging, sensing, and antenna-coupled quantum light sources. In this work, we use a custom-designed superconducting nanowire single-photon detector to directly read out the near-field interaction between a source and a detector. We use a subwavelength-sized aperture at the end of an optical fiber to record spatial near-field maps and to measure the distance dependence of the optical near-field interaction. Our measurements can be well described by a superposition of evanescent source fields with no noticeable probe-sample coupling. Our approach is a first step towards the development of near-field imaging techniques with single quantum sensitivity. *Published by AIP Publishing*. https://doi.org/10.1063/1.5037964

The quantum nature of optical near-fields has been of interest for years.[1–3] Recent studies focused on the coupling of optical antennas to single-photon detecting devices,[4–7] the detection of single plasmons,[8] and the characterization of single-photon detection in nanoscale environments.[9,10]

A single photon detector records the arrival of photons, quanta of propagating electromagnetic radiation. Propagating radiation is transverse and it is decoupled from the source that generated it. On the other hand, optical near-fields are intimately coupled to their sources. Consequently, when a single photon detector interacts with an optical near-field, the detector's clicks represent quanta of the electromagnetic interaction between source and detector and *not* the electromagnetic field *per se*.[1,11,12] The near-field interaction can be seen as an energy transfer process mediated by virtual photons.[3]

For the investigation of optical near-fields, we use a Superconducting Nanowire Single-Photon Detector (SNSPD)[13,14] fabricated in the form of a subwavelength-sized area[15] and place it close to a subwavelength aperture, at a distance of a few nanometers. No propagating radiation is involved in the detection process. In addition to characterizing the properties of the near-field interaction, the ability to directly probe evanescent fields, without the need to scatter the evanescent field into propagating radiation, is a promising approach for improving the sensitivity of scanning near-field optical microscopy (SNOM) and for expanding the applications of this technique. The presented work is a step towards developing a nanoscale single-photon detector integrated onto a scanning tip.[16–18]

A sketch of the experiment is shown in Fig. 1(a). The SNSPD is operated at a bias current of approximately 7 μA. The electrical pulses generated by the near-field interaction are amplified by two wide-band RF amplifiers connected in series and converted to TTL digital standard with an adjustable threshold discriminator. The detector used in this work, shown in Fig. 1(b), is a $200 \times 200\,\mathrm{nm}^2$-area constriction in a 6 nm-thick NbTiN film. The device is fabricated on a sapphire substrate by magnetron sputtering thin-film deposition followed by electron beam lithography and reactive ion etching.

Before using the constricted SNSPD for near-field measurements, we have investigated its performance under diffraction-limited laser illumination using a cryogenic objective. The critical temperature is found to be $T_c = 7.5$ K, measured at a bias current of $I_b = 0.1$ μA. We use a 20 mW laser diode emitting at a wavelength of 700 nm and a set of optical neutral density filters to attenuate the laser light. The minimum power level is 3 fW. The light is focused onto the constricted area of the device, to a spot of 1 μm in size.

For bias currents below $I_b = 10$ μA, only the constriction in the center of the device is detecting light. To determine the detection efficiency, we record the count rate as a function of laser power and use a calibrated avalanche photodetector as a reference. We find that the detection efficiency is $\sim$1% in the power range from 3 fW to 330 pW. In order to measure the dark-count rate of the device, we repeat the same procedure with the laser and all other light sources switched off, and the cryostat's optical windows blocked with a few layers of aluminum foil. The dark-count rate at bias currents lower than $I_b = 15$ μA was found to be lower than 1 Hz.

The detector is installed on a custom-built piezoelectric positioning stage. The stage together with the detector and the aperture probe is placed inside a bath cryostat and submerged in superfluid helium at a temperature of approximately 2 K. Once cold, the aperture probe is positioned directly on top of the SNSPD nanowire constriction. The aperture probes are fabricated by chemical etching of a glass

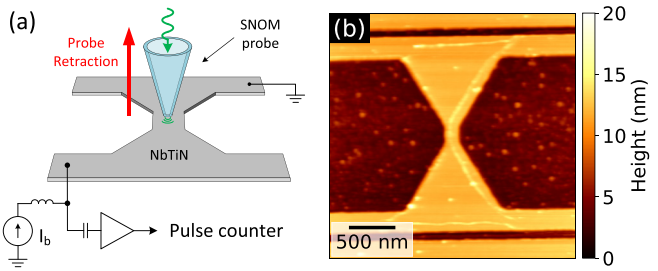

FIG. 1. (a) Illustration of the experiment. A subwavelength aperture acts as the source of the optical near-field. The aperture is placed in close proximity over an SNSPD. Detector clicks are recorded as a function of the aperture position. (b) Atomic force microscopy (AFM) image of the SNSPD. The device features a $200 \times 200\,\mathrm{nm}^2$ constriction in a 6 nm-thick NbTiN film deposited on sapphire substrate. The pattern was fabricated by electron beam lithography followed by reactive ion etching.

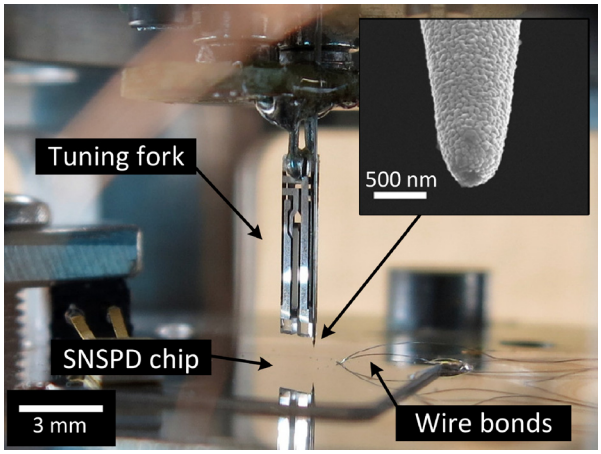

FIG. 2. A close-up photograph of the experimental configuration. The SNOM aperture probe is attached to a quartz tuning fork and positioned above the SNSPD chip. The inset shows a scanning electron microscopy image of a SNOM aperture probe.

fiber and subsequent Al evaporation. The probe-sample distance is sensed with a quartz tuning-fork based FM shear-force feedback mechanism[19,20] and maintained constant with a piezoelectric tube actuator. The tracking of the tuning fork resonance frequency is realized with a commercial phase-locked loop. The control of the probe (positioning and scanning) is handled by a commercial controller.

Figure 2 shows a photograph of the SNSPD detector chip underneath the SNOM probe attached to a quartz tuning fork. In the research presented in this paper, two different types of aperture probes and wavelengths were used. For distance-dependent near-field measurements, we used a wavelength of 532 nm, and for near-field imaging, we used a wavelength of 700 nm. The power at the input of the SNOM fibers was approximately 0.5 mW in both cases.

After cooling the experimental setup and submerging it in superfluid helium, we approach the aperture probe to the SNSPD and record raster-scan images while maintaining a constant probe-sample separation of a few nanometers. While scanning, we record the rate of pulses generated by the SNSPD detector. This allows us to record the spatial sensitivity distribution of the detector surface with subdiffraction resolution. Simultaneously we record the corresponding topographical map. Figure 3 shows $1 \times 1\ \mu m^2$ images of the SNSPD constriction zone for both the count rate and topography. The two images were recorded in superfluid helium

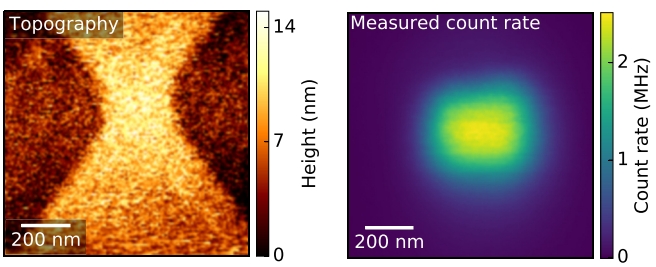

FIG. 3. Topography (left) and count rate (right) images of the SNSPD constriction area acquired by raster-scanning the SNOM probe over the surface of the SNSPD. The two images were acquired simultaneously in superfluid helium at a temperature of 2 K using a SNOM probe with a 220 nm-size aperture.

with a 220 nm-size aperture probe. The acquired images confirm that the SNSPD detector is light-sensitive only in the nanowire constriction area as it is expected, and that the SNOM probe can be accurately positioned in the center of that area. The positioning accuracy needed for the distance-dependent measurements is discussed in the next paragraph.

The count rate of the pulses recorded at the output of the SNSPD detector represents the strength of the near-field interaction between the source (aperture probe) and the detector (SNSPD nanowire). By positioning the SNOM probe in the center of the nanowire constriction and retracting it away from the surface of the sample, we record the distance dependence of the near-field interaction. As shown in Fig. 4, we observe a nearly-exponential decay, characteristic of an evanescent wave.

To theoretically describe the measured behavior, we model the source by a uniform in-plane electric field E_0 constrained to a circular area of radius w_0 located in the plane $z = 0$. Following Novotny and Hecht,[21] the field spreads out as

$$E_x(\rho, z) = E_0 \frac{w_0^2}{2} \int_0^\infty \mathrm{e}^{-k_\parallel^2 w_0^2/4}\, k_\parallel\, J_0(k_\parallel \rho)\, \mathrm{e}^{\mathrm{i}k_z z} dk_\parallel, \qquad (1)$$

where J_0 is the Bessel function of the first kind, $k_\parallel = \sqrt{k_x^2 + k_y^2}$ is the in-plane spatial frequency, and k_z is the spatial frequency perpendicular to the aperture plane

$$k_z = \sqrt{\left(\frac{2\pi}{\lambda}\right)^2 - k_\parallel^2}. \qquad (2)$$

For an aperture of a size much smaller than the wavelength of illuminating radiation k_z is mainly imaginary. Therefore, the field behind the aperture is primarily composed of non-propagating near-fields that decay exponentially from the aperture plane.

In Fig. 4, we superimpose the intensity of the field (1) to the measured detector count rate. An excellent agreement between the theory and experiment is obtained. The fitting parameters are the aperture size w_0 and the field intensity in

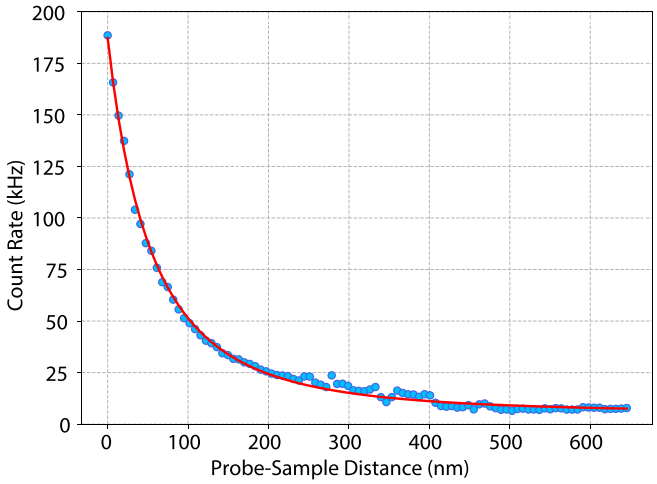

FIG. 4. Dependence of the optical near-field interaction on probe-sample distance. Dots are measurements and solid lines are theoretical fits. The aperture probe was retracted from the sample at a speed of 50 nm/s.

the aperture plane E_0 (related to the maximum count rate at the shortest probe-sample distance). The field decays exponentially, and the aperture radius resulting from the fitting process is $w_0 = 94\,\text{nm}$. The aperture radius is in agreement with the probe specifications and corresponds to $\lambda/5.66$ for a wavelength of 532 nm.

The results shown in Fig. 4 seem to indicate that the SNSPD clicks represent the field of the source and that the SNSPD acts as a passive probe. We observe no measurable backaction from the detector on the source, which would result in interference undulations, akin to Fabry-Pérot resonances with a period of $\lambda/2 = 266\,\text{nm}$. We verified that such interference undulations do exist for near-field probes with larger aperture size and hence larger contribution of far-field radiation. Furthermore, evanescent coupling between the probe and sample should have its signature in a flattening of the distance dependence at small distances, as is the case in frustrated total internal reflection.[21] No such behavior is observed in our data shown in Fig. 4. Thus, our data can be best described by a superposition of exponentially decaying near-fields and the contribution of probe-sample coupling can be largely ignored.

In this work, we measured the optical near-field interaction between a source and a detector. We used a custom, subwavelength-size SNSPD detector directly interacting with a subwavelength aperture of a SNOM probe. We record spatial near-field maps and measure the distance dependence of the near-field interaction at a temperature of 2 K. We find that the detector signal can be well described by a superposition of evanescent source fields and that the backaction on the source can be neglected. The experimental platform developed in this research can be used for further investigation of the quantum nature of optical near-field interactions and is a step towards the integration of a subwavelength single-photon detector on a scanning tip.

We thank Andreas Schilling, Andreas Engel, and Martin Frimmer for valuable support and fruitful discussions. This work has been supported by ETH Grant No. ETH-07 16-1.

[1]C. Carniglia and L. Mandel, "Quantization of evanescent electromagnetic waves," Phys. Rev. D **3**, 280–296 (1971).
[2]J. Vigoureux, L. D'Hooge, and D. Van Labeke, "Quantization of evanescent electromagnetic waves: Momentum of the electromagnetic field very close to a dielectric medium," Phys. Rev. A **21**, 347–355 (1980).
[3]D. L. Andrews and D. S. Bradshaw, "Virtual photons, dipole fields and energy transfer: A quantum electrodynamical approach," Eur. J. Phys. **25**, 845–858 (2004).
[4]R. M. Heath, M. G. Tanner, T. D. Drysdale, S. Miki, V. Giannini, S. A. Maier, and R. H. Hadfield, "Nanoantenna enhancement for telecom-wavelength superconducting single photon detectors," Nano Lett. **15**, 819 (2015).
[5]X. Hu, E. A. Dauler, R. J. Molnar, and K. K. Berggren, "Superconducting nanowire single-photon detectors integrated with optical nano-antennae," Opt. Express **19**, 17–31 (2011).
[6]M. Csete, Á. Sipos, A. Szalai, F. Najafi, G. Szabó, and K. K. Berggren, "Improvement of infrared single-photon detectors absorptance by integrated plasmonic structures," Sci. Rep. **3**, 2406 (2013).
[7]Q. Wang, J. J. Renema, A. Engel, and M. J. A. de Dood, "Design of nbn superconducting nanowire single-photon detectors with enhanced infrared detection efficiency," Phys. Rev. Appl. **8**, 034004 (2017).
[8]R. W. Heeres, S. N. Dorenbos, B. Koene, G. S. Solomon, L. P. Kouwenhoven, and V. Zwiller, "On-chip single plasmon detection," Nano Lett. **10**, 661–664 (2010).
[9]A. Engel, J. Lonsky, X. Zhang, and A. Schilling, "Detection mechanism in SNSPD: numerical results of a conceptually simple, yet powerful detection model," IEEE Trans. Appl. Supercond. **25**, 1–7 (2015).
[10]J. Renema, Q. Wang, R. Gaudio, I. Komen, K. op 't Hoog, D. Sahin, A. Schilling, M. van Exter, A. Fiore, A. Engel, and M. de Dood, "Position-dependent local detection efficiency in a nanowire superconducting single-photon detector," Nano Lett. **15**, 4541–4545 (2015).
[11]E. A. Power and T. Thirunamachandran, "Analysis of the causal behavior in energy transfer between atoms," Phys. Rev. A **56**, 3395–3408 (1997).
[12]O. Keller, *Quantum Theory of Near-Field Electrodynamics, Nano-Optics and Nanophotonics* (Springer, Berlin, Heidelberg, 2012).
[13]G. Gol'tsman, O. Okunev, G. Chulkova, A. Lipatov, A. Dzardanov, K. Smirnov, A. Semenov, B. Voronov, C. Williams, and R. Sobolewski, "Fabrication and properties of an ultrafast NbN hot-electron single-photon detector," Appl. Supercond. , IEEE Trans. **11**, 574–577 (2001).
[14]C. Natarajan, M. Tanner, and R. Hadfield, "Superconducting nanowire single-photon detectors: Physics and applications," Supercond. Sci. Technol. **25**, 063001 (2012).
[15]D. Bitauld, F. Marsili, A. Gaggero, F. Mattioli, R. Leoni, S. J. Nejad, F. Lévy, and A. Fiore, "Nanoscale optical detector with single-photon and multiphoton sensitivity," Nano Lett. **10**, 2977–2981 (2010).
[16]Q. Wang and M. de Dood, "An absorption-based superconducting nano-detector as a near-field optical probe," Opt. Express **21**, 3682–3692 (2013).
[17]Q. Wang, J. Renema, A. Engel, M. van Exter, and M. de Dood, "Local detection efficiency of a nbn superconducting single photon detector explored by a scattering scanning near-field optical microscope," Opt. Express **23**, 24873 (2015).
[18]O. Hayden, R. Agarwal, and C. Lieber, "Nanoscale avalanche photodiodes for highly sensitive and spatially resolved photon detection," Nat. Mater. **5**, 352–356 (2006).
[19]K. Karrai and R. Grober, "Piezoelectric tip-sample distance control for near field optical microscopes," Appl. Phys. Lett. **66**, 1842–1844 (1995)..
[20]W. Atia and C. Davis, "A phase-locked shear-force microscope for distance regulation in near-field optical microscopy," Appl. Phys. Lett. **70**, 405–407 (1997).
[21]L. Novotny and B. Hecht, *Principles of Nano-Optics*, 2nd ed. (Cambridge University Press, Cambridge, 2012).